



# Effects of drying pretreatment on microwave pyrolysis characteristics of tobacco stems

Hang Gao<sup>1,2,3</sup> · Jing Bai<sup>1,2,3,4</sup> · Yuanxia Wei<sup>1,3</sup> · Wencheng Chen<sup>1</sup> · Lefei Li<sup>1</sup> · Guilin Huang<sup>1</sup> · Pan Li<sup>1,2,3</sup> · Chun Chang<sup>2,3,4</sup>

Received: 10 July 2021 / Revised: 19 September 2021 / Accepted: 18 November 2021 / Published online: 11 January 2022  
© The Author(s), under exclusive licence to Springer-Verlag GmbH Germany, part of Springer Nature 2021

## Abstract

In this work, the effect of volumetric drying and surface drying pretreatment on microwave pyrolytic characteristics of tobacco stems was investigated. The microwave oven was used for volumetric drying with different power outputs, while the electric oven was used for surface drying at 105°C. The biomass dried using microwave drying was compared with the dried using oven drying, and the yields and properties of solids, liquids, and gases were determined. Besides, the decomposition mechanism of nicotine was preliminarily expounded. The results showed that the drying rate of microwave could reach up to 1.093 g m<sup>-2</sup> s<sup>-1</sup>, which was approximately 5 times the maximum drying rate of oven. There was little change in the yield of biochar, and the yield of bio-oil increased, while the yield of non-condensable gas decreased by microwave compared to oven. When microwave drying was used, the concentration of CO<sub>2</sub> in the pyrolysis gas was higher, but the yields of H<sub>2</sub>, CO and CH<sub>4</sub> were lower. The preliminary analysis of pyrolytic bio-oil revealed that the relative content of alcohols, acids, aldehydes, and ketones increased to 6.46%, 3.39%, 18.59%, and 18.18%, and the relative content of phenols decreased to 8.74% by microwave. After oven drying, the residence time of volatiles in the reaction zone increased during the pyrolytic process, and nicotine was thermally decomposed at high temperatures and combined with other free radicals; the relative contents of nicotine in the bio-oil have decreased from 11.78 to 6.55%. Microwave drying decreased the water content of bio-oil. At the same time, the stability of bio-oil improved. Therefore, microwave drying is an economical pretreatment method for biomass fast pyrolysis.

**Keywords** Tobacco stem · Microwave pyrolysis · Drying characteristics · Pyrolytic products

## 1 Introduction

The United Nations held its 75th session of the General Assembly in New York, September 22, 2020. On the Paris Agreement, China, the European Union, Japan, Korea, and other countries had made a series of solemn commitments and set a target of net zero emissions and carbon neutrality.

As a “zero carbon energy,” biomass energy is one of the most important renewable energy for human beings. It is a renewable energy that can be stored. Biomass is the organic material contained in all living bodies, including plants, animals, and microorganisms.

Tobacco stems are a common biomass; they are the thick and hard veins of tobacco leaves and account for about 25 to 30% of the leaf weight. As a major tobacco producer, China has the largest tobacco market in the world. The annual output of tobacco stems is about 600,000 tons; only two-thirds are used for cigarette production. The remaining hundreds of thousands of tons of tobacco stems are discarded. In addition to causing a waste of resources, the alkali metal components in tobacco stems entering the soil can also pollute water sources. How to clean and efficiently use waste tobacco stems not only has an important significance to the environment, but also can create good economic benefits. Pyrolysis is one of the most effective methods. Pyrolysis is one of the

✉ Jing Bai  
baijing8279@163.com

<sup>1</sup> School of Mechanical and Power Engineering, Zhengzhou University, Zhengzhou 450001, China

<sup>2</sup> Henan Outstanding Foreign Scientists' Workroom, Zhengzhou 450001, China

<sup>3</sup> Engineering Laboratory of Henan Province for Biorefinery Technology and Equipment, Zhengzhou 450001, China

<sup>4</sup> School of Chemical Engineering, Zhengzhou University, Zhengzhou 450001, China

thermochemical conversion technologies of biomass, and it is also the prime method of biomass resource utilization. It is carried out at the mild conditions of high temperature and atmospheric pressure. Through pyrolysis, biomass can be transformed into three species of products: biochar can be used as adsorption material [1], catalyst carrier [2], etc.; non-condensable gas can be used as fuel [3]; bio-oil can be used as liquid fuel [4] or extracted high-value products [5–8] from bio-oil. Nevertheless, the high moisture content of bio-oil will degrade its quality. Therefore, lowering the moisture content of biomass is an important step in biomass pyrolytic process [9].

There are three forms of water in biomass [10]: water vapor in pores, dissociative liquid water in pores and capillaries, and bound water in solid structures. The moisture content in biomass will debase the quality of pyrolytic bio-oil, resulting in more energy loss during combustion [11]. Two drying methods are considered here: conventional oven drying for surface heating and microwave drying for volumetric heating [12]. Oven drying transfers the heat to the surface of the biomass through heat convection, heat radiation, etc., and then the heat is transferred to the inside of biomass. A temperature gradient is existed inside the biomass, which lowers the drying efficiency, and it cannot effectively remove the moisture inside biomass, and it also has high requirements on the particle size of biomass. However, microwave overcomes these disadvantages of oven drying, so microwave technology is also used extensively in the field of drying [13, 14]. In recent years, researchers have applied microwave drying to the field of biomass drying pretreatment [15–17]. Compared with oven drying, microwave drying has high heating efficiency and can heat all parts of the biomass simultaneously; it can be automatically controlled by switches or programs with no thermal inertia. Microwave drying technology originated in the 1940s and began to be widely used in foreign countries in the 1960s. The research of microwave drying technology in China started relatively late, and the application began in the early 1970s. Up to now, although the research time of microwave drying biomass is comparatively short, the study had been developed rapidly, and many achievements had been obtained. The effect of microwave drying on characteristics of two different types of biomass namely rice straw and Chinese pennisetum had been investigated; they found that the energy density of dried biomass is 14% higher than that of undried biomass; in addition, the calorific value of biomass after drying also increased, while H/C and O/C decreased [18]. A study on the microwave drying of lignite had been performed to the functional group changes and pyrolytic characteristics; it was found that the number of oxygen-containing functional groups of lignite was lowered after microwave drying, and the yield of polycyclic aromatic hydrocarbons was also lowered down in pyrolytic products [19]. The effect of microalgae mass

and microwave power on drying characteristics had been performed. They achieved a maximum drying efficiency of 76%, at the condition of 130 g of the microalgae with a microwave power of 630 W [20]. In a study about the effects of different microwave powers on the pyrolytic characteristics of pine sawdust, peanut hulls, and corn stalks, the results indicated that microwave drying could enhance the porosity of biomass, and promote the production of liquid products during the pyrolysis process [21]. To sum up, microwave drying has the advantage of high drying efficiency and promotes the quality of liquid products, these characteristics has attracted people's attention.

In recent years, researchers also have conducted a lot of research on tobacco stems. A thermogravimetric analyzer had been used to study the pyrolytic process of tobacco stems in a nitrogen atmosphere [22]. Chen [23] studied the effect of hydrochloric acid pickling pretreatment on the pyrolytic characteristics of tobacco stems. Liu [24] used the PY-GC/MS to study the pyrolytic products at low and high temperature of tobacco stems. Yan [25] investigated the effect of pyrolytic temperature on the components of bio-oil.

As could be summarized, researchers had conducted in-depth research on the changes in pyrolytic conditions, and the effects of different solvent washing pretreatments on the pyrolysis of tobacco stems, as well as the pyrolytic kinetics and thermodynamics of tobacco stems. Microwave drying was less used in the field of biomass pretreatment, and the research on the effect of microwave drying on the microwave pyrolytic characteristics of tobacco stems had hardly been reported. Moreover, the physical and chemical properties of the biomass after microwave pretreatment had also undergone some changes [25–27]. Therefore, this work selects waste tobacco stems as experimental materials, and studies the effects of microwave drying and oven drying on the physical and chemical properties of tobacco stems and the pyrolytic products of microwave pyrolysis.

## 2 Experiment

### 2.1 Materials

In this work, the tobacco stems (TS) were used as the pyrolytic material with high content of nicotine, which came from Pingdingshan City, Henan Province, China. Silicon carbide particles (SiC) were used as the microwave adsorptive material. A high-speed pulverizer was used to pulverize the TS and screened out particles with 20 and 40 mesh. The industrial analysis of TS was done according to the national standard GB/T 28731–2012 of the People's Republic of China, and an elemental analyzer (vario el III, Elementar) was used to analyze the element content of TS samples.

**Table 1** The elemental analysis and industrial analysis of TS

Elemental analysis/wt (%)					Industrial analysis/wt (%)			
C <sub>ad</sub>	H <sub>ad</sub>	O <sub>ad</sub>	N <sub>ad</sub>	S <sub>ad</sub>	M <sub>ad</sub>	A <sub>ad</sub>	V <sub>ad</sub>	FC <sub>ad</sub>
37.62	4.25	40.11	2.23	1.15	17.85	18.12	52.92	11.11

**Table 2** The elemental atomic ratio of conventional biomass

	TS	Corn stalk [28]	Wheat straw [29]	Rice straw [30]	Cotton straw [30]
H/C <sup>ar</sup>	1.36	1.65	1.36	1.76	1.64
O/C <sup>ar</sup>	0.80	0.75	0.59	0.78	0.74

ar atomic ratio

Table 1 shows the elemental analysis and industrial analysis of TS. It could be seen from Tables 1 and 2, compared with the traditional biomass corn stalk, wheat straw, rice straw, and cotton straw, that there were no too big differences about the contents of C, H, and O. But the N content in the TS composition was higher, at 2.23%, because nicotine is a nitrogenous compound which is peculiar to TS. The O/C was higher than the traditional biomass, which increased the polarity of bio-oil and lowered the calorific value of the bio-oil. Both drying and torrefaction can remove the moisture in biomass, reduce oxygen content, and improve the quality of bio-oil. The low S content of TS revealed the clean characteristics of TS as biomass energy. The high volatile content indicated that the TS had the property suitable for thermochemical conversion. High ash content indicated that TS had a larger space for a thermochemical upgrading.

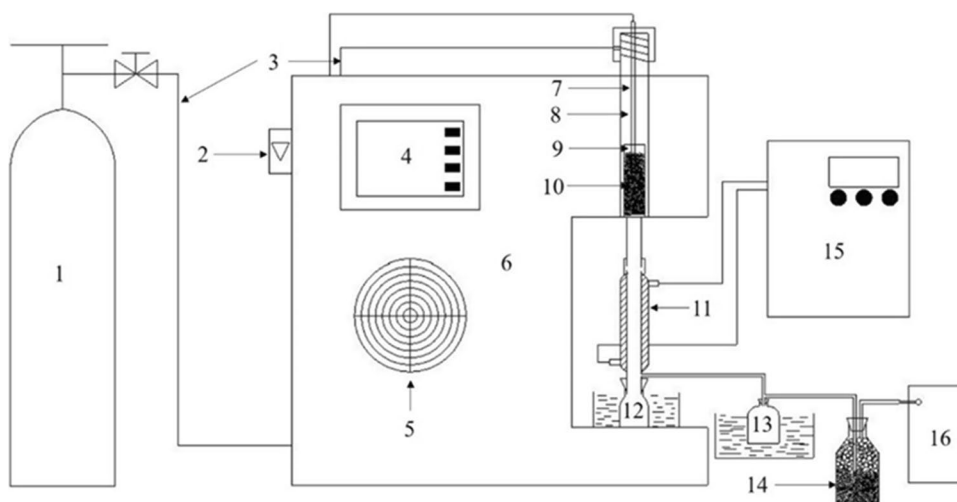
## 2.2 Drying pretreatments

An electric oven was used for conventional oven drying (Shuli) and represented the surface heating. A household microwave oven (M1-L213B, Media) was used for microwave drying (MD) and represented the volumetric heating. Three powers of 380 W, 540 W, and 700 W were used for MD. 4g TS in a crucible was put into the microwave oven, then adjust the microwave power for drying, took out once per minute and weighed them with electronic balance at a sensitivity of 0.001 g, and calculated the moisture loss with subtraction method; the weighing should be completed within 10 s. In order to ensure the repeatability of the drying data, each power drying experiment was done three times and averaged. The oven drying (OD) step was the same as above, carried out in an electric oven, and the drying temperature was 105 °C, as a control. Also, the microwave pyrolysis of untreated TS was used as the control group.

## 2.3 Device and steps

A vertical microwave catalytic reactor was used for pyrolysis (Fig. 1). Firstly, TS and SiC particles were weighed, then mixed them evenly in the quartz hanging basket, put the basket into the quartz tube, inserted the thermocouple, and sealed the quartz tube. High-speed nitrogen was used for 10 min to purge the air in the pipeline. The pyrolytic temperature was set at 550 °C and pyrolyzed TS for 10 min with

**Fig. 1** Microwave pyrolytic experimental device. 1, Nitrogen bottle; 2, rotameter; 3, nitrogen pipeline; 4, control system; 5, fan; 6, vertical microwave catalytic reactor; 7, thermocouple; 8, quartz tube; 9, quartz hanging basket; 10, sample; 11, condenser tube; 12, oil collection bottle; 13, oil collection bottle; 14, gas washing bottle; 15, cold trap; 16, air bag



the nitrogen flow rate at 0.25 L/min. The volatiles were taken out of the quartz tube by nitrogen and condensed through the condensing tube. The glass bottle was placed in the ice water bath to collect the liquid product. The non-condensing gas was collected by the air bag at the tail, through a washing cylinder to remove the incomplete cooled oil and water vapor.

## 2.4 Analytical methods

A thermogravimetric analyzer (SDT650, TA) was used to analyze the samples of different drying methods. The analysis was in a nitrogen environment with a temperature rate of 30 °C/min from 50 to 1200 °C.

The BK100-01 automatic specific surface area and pore analyzer of Beijing Jingwei Gaobo Technology Co., Ltd. was used to determine the pore structure parameters of dried samples and biochar; the dried samples and biochar were degassed in vacuum at respectively 100°C and 300°C for 5 h, and the nitrogen isothermal adsorption and desorption method was used to analyze the samples in a 77 K liquid nitrogen environment.

A Fourier Transform Infrared Spectrometer (TENSOR II, Bruker) was used to test the functional groups of biochar. The biochar and KBr were placed in an oven at 105 °C and 120 °C for 6 h to remove moisture. The biochar and KBr were ground and mixed with a ratio of 1:99, then compressed into tablets, and the samples were analyzed in spectral analysis range of 400 to 4500  $\text{cm}^{-1}$  with resolution of 1  $\text{cm}^{-1}$ .

A desktop scanning electron microscope (JCM-6000PLUS, JEOL) was used to analyze the surface characterization and morphology of dried samples and biochar, and the magnification was 1000 times. Because of the weak electrical conductivity of dried samples, they were sprayed with metal before analysis.

A gas chromatography/mass spectrometer (GC-8860/MS-5977A, Agilent) was used to analyze the bio-oil. The instrument conditions used for the measurement are as follows: (1) GC conditions: chromatographic column was of HP-5MS (30 m  $\times$  0.25 mm  $\times$  0.25  $\mu\text{m}$ ), carrier gas was He, gas flow rate was 1.2 mL/min, the split ratio was 50:1, injection volume was 0.2  $\mu\text{L}$ , the temperature of the injector was 290 °C, column heating program was that the initial temperature was 40°C, kept for 4 min, and then the temperature was raised to 280°C at the rate of 5°C/min and kept for 5 min; (2) MS conditions: MS interface temperature was 290°C, scanning range was from 40 to 500 (m/Z), and solvent delay time was 2 min.

A gas chromatograph (GC-14C, Shimadzu Corporation) was used to analyze the non-condensable gas. Standard gas control procedure was firstly used to identify the gas species, and the external standards were used to quantitatively analyze the main components of gas products ( $\text{CO}$ ,  $\text{CO}_2$ ,  $\text{H}_2$ ,  $\text{CH}_4$ ).

## 3 Results and discussion

### 3.1 Drying characteristic analysis

In the drying process of TS, the drying rates at different moments were calculated by measuring the volatilized moisture content of TS in per a same time period, as shown in Fig. 2. The formula for calculating the drying rate was as follows:

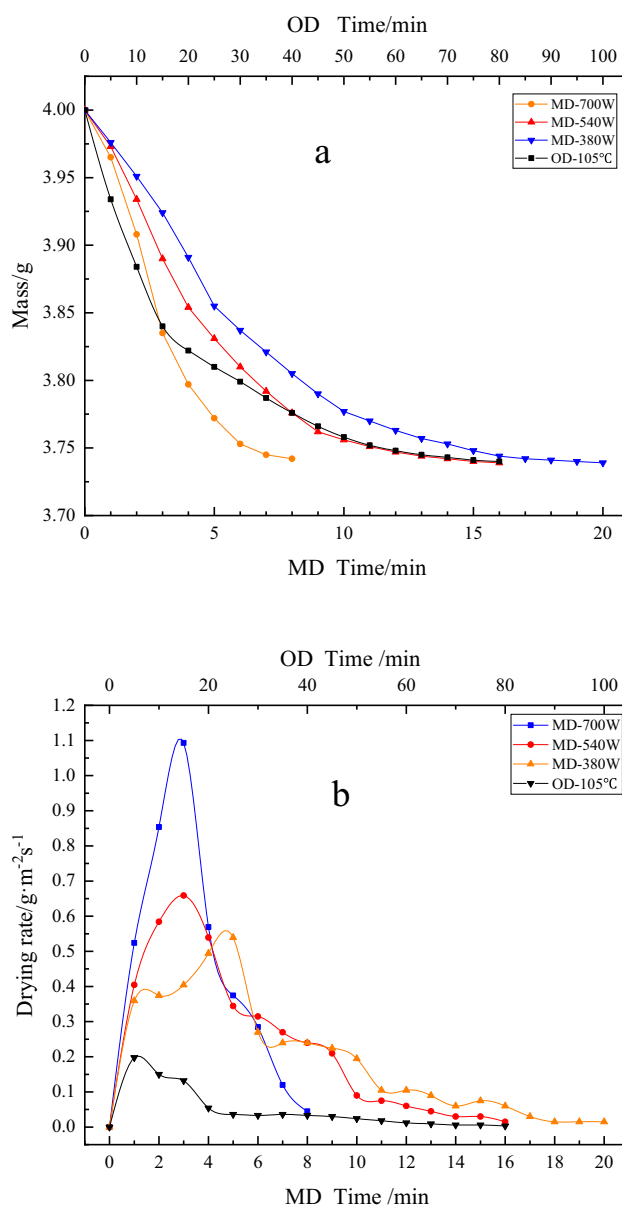


**Fig. 2** a The weight loss curve, (b) the drying rate curve of MD and OD

**Table 3** The specific surface area of TS

	BET surface area(m <sup>2</sup> /g)
OD	0.081
MD	1.216
ascontrol	0.106

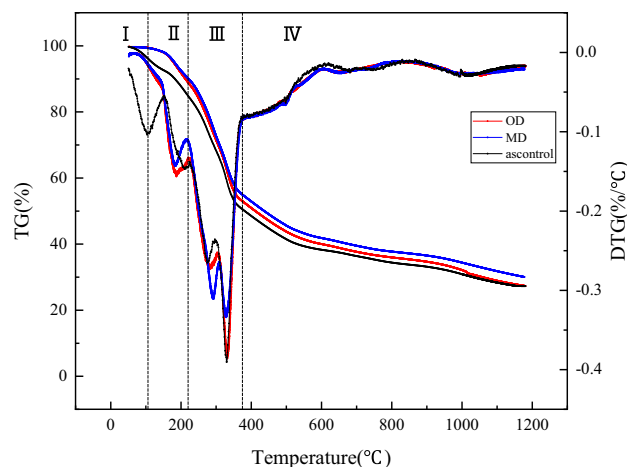
$$M_{DR} = \frac{\Delta M}{A\Delta t} \tag{1}$$

where  $M_{DR}$  is the drying rate, g m<sup>-2</sup> s<sup>-1</sup>;  $\Delta M$  is the volatilized moisture mass from TS, g;  $A$  is the total surface area of TS particles, m<sup>2</sup>; and  $\Delta t$  is the same time period, s.

For MD, due to the strong polarity of water molecules, which caused the ability to absorb microwave energy of water was very strong, so in the process of microwave heating, the loss of TS mass was equal to the loss of water [21]. As shown in Fig. 2, when dried with the oven, the mass of TS tended to be stable with the volatilization of moisture, but MD was different, and its drying end was usually difficult to distinguish. When the moisture was almost completely evaporated, other substances began to absorb microwave energy and the heat accumulated inside the biomass over time resulted in the temperature of the biomass to rise rapidly, and then the biomass began to pyrolyze or burn. There was no obvious boundary between physical drying and chemical reaction.

It could be observed from Fig. 2 that the drying rate of MD could reach up to 1.093 g m<sup>-2</sup> s<sup>-1</sup>, which was approximately 5 times the maximum drying rate of OD, and the second half of the MD curve tended to coincide with that of the OD when the microwave power was at 540 W. Under the condition of same moisture loss rate, the time MD cost at 540 W was one-fifth of OD at 105°C. When the microwave power was at 700 W, the time required was only about one-tenth of OD. The microwave power was too high and, however, made the TS begin to decompose. As mentioned above, the second half of the MD curve at 540 W tended to coincide with the OD. Therefore, MD at 540 W and OD at 105°C were chosen for subsequent pyrolysis experiments.

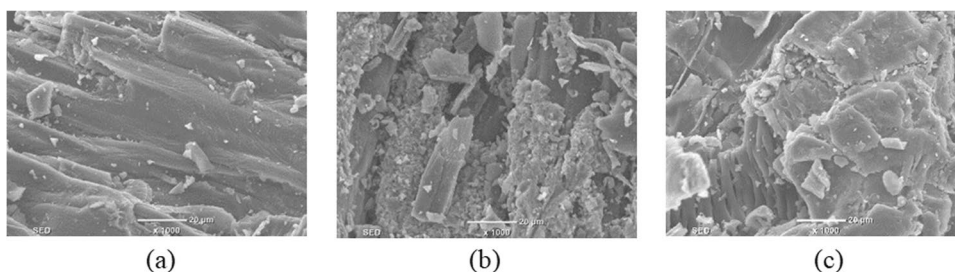
Seen from Fig. 2, MD and OD processes were divided into three stages: the accelerated stage, the moderative stage,



**Fig. 4** TG-DTG curves of different drying methods

and the constant speed stage. The initial stage depended on both internal and external mass transfer rates, and the drying rate increased over time [27], while the second and third stages depended on internal mass transfer resistance and solid-water interaction [31]. For MD, when the microwave power was too high, the constant speed stage was not obvious. Compared with OD, the MD rate was higher and the drying time was shorter, which meant that the moisture inside the TS was quickly transferred to the surface and released, and more internal pores were formed. Therefore, a specific surface area analyzer and a scanning electron microscope were used to test and analyze the TS of MD and OD. The results are shown in Table 3 and Fig. 3. MD increased the specific surface area of TS. It could be seen from the SEM images of TS that the rapid evaporation process of moisture using MD expanded the internal pores of TS, and significantly destroyed the surface structure of TS, with smaller structural fragments covering the surface and increased the size of the surface pores. These changes were conducive to the rapid heating and decomposition of TS, and the rapid precipitation of pyrolytic gas when heated thus affected the distribution of pyrolytic products, which also proved that MD increased the porosity of TS.

**Fig. 3** The SEM images of TS: (a) OD, (b) MD, and (c) ascontrol



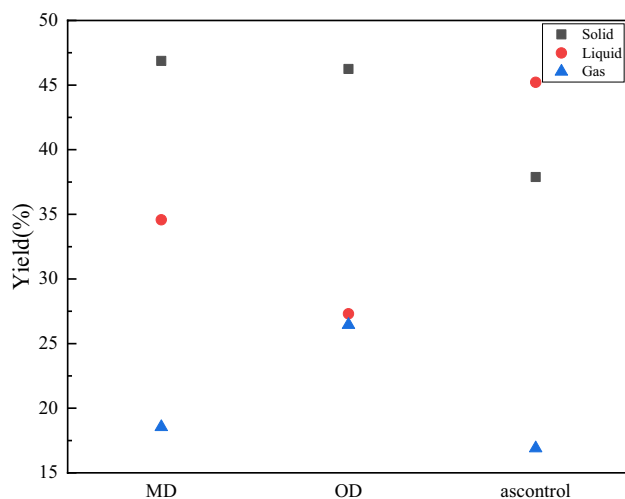


**Fig. 5** Three phase yield of TS microwave pyrolysis

**Table 4** The pore properties of TS microwave pyrolytic biochar

	BET surface area (m <sup>2</sup> /g)	Pore volume (cm <sup>3</sup> /g)	Average pore diameter (nm)
OD	9.926	0.028	38.014
MD	3.624	0.019	20.515
ascontrol	5.912	0.027	14.035

### 3.2 Thermogravimetric analysis

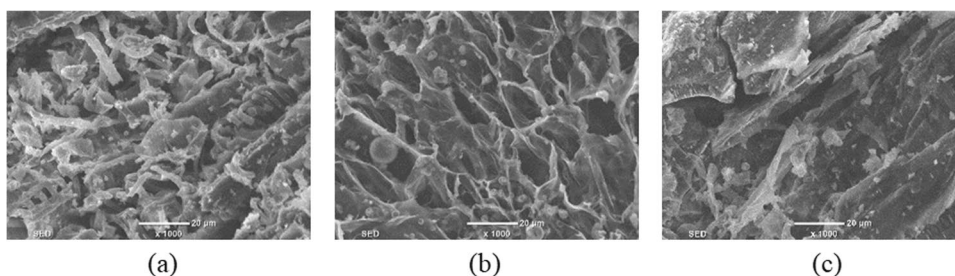
To investigate the effect of MD on the pyrolytic behavior of dried samples, the TG and DTG curves of MD and OD were compared, and the untreated TS served as a control group. The results are shown in Fig. 4. It could be observed from Fig. 4 that the TG-DTG curves' change trends of different drying methods were similar, which indicated that MD rarely affected the pyrolytic mechanism; it just changed the peak value of the curve. However, in the area I, the DTG curve of control group is different from OD and MD, which is the reason of water evaporation. The pyrolytic process of TS was divided into the following four stages: (1) the drying stage (50~120°C). This stage was the process of absorbing heat and removing moisture from the TS. There were no chemical reactions, and

the chemical composition was basically unchanged. There was only a slight decrease, and the weight becomes 99% of the original mass. During this process, the heat absorption state was always present. (2) The second is the preheating cracking stage (120~220°C). From this stage, the TS began to undergo chemical changes, and the composition and structure of TS began to change. The hemicellulose with the lowest initial temperature of pyrolysis (180~285°C) began to decompose slightly with the increase of temperature, and broke the connection between lignin and cellulose [32]. (3) The third is the rapid pyrolytic stage (220~375°C). This stage was the main stage of pyrolysis. In this temperature range, about 60~70% of the volatile matter in the entire temperature section was precipitated, and at this stage, the DTG curve had obvious main peak and shoulder peak. The peak temperature of the main peak was 330 °C, and the peak of the shoulder peak was 290 °C. This stage was caused by the pyrolysis of the three major organic components of biomass (cellulose, hemicellulose, and lignin). The pyrolytic temperature range of lignin was 269~388°C [33]. Hemicellulose was basically decomposed at 290°C, and cellulose was basically decomposed at 330°C. Lignin had the best thermal stability (365~500°C) [34]; there will be a major degradation stage at 320~400°C [22]. (4) The residue was slowly pyrolyzed (375~1200°C); the TG curve at this stage showed a slow downward trend. The peak temperature is 443 °C; during this stage, the lignin in the TS mainly undergone the secondary cracking, and the overall weight loss tended to be flat.

### 3.3 Effect of microwave drying on microwave pyrolysis of TS

The yields of pyrolytic products of TS were calculated to investigate the effect of MD on microwave pyrolytic products. As shown in Fig. 5, both MD and OD reduced the yields of bio-oil, because the water contained in the untreated TS also accounted for a considerable proportion in the bio-oil, resulting in a large increase in the yield of liquid products. Moreover, the yield of bio-oil increased and the yield of non-condensable gas decreased using MD, compared to OD. This was due to the MD pretreatment increasing the total pore volume inside the TS particles, so the residence time of the volatiles in the TS and the reactor decreased, and also the intensity of the volatile

**Fig. 6** SEM images of biochar: (a) OD, (b) MD, and (c) ascontrol



matter’s secondary cracking reaction. The volatiles generated more biochar and non-condensable gas in the secondary cracking reaction, and the yield of biochar and gas increased [35]. However, from the results, the yield of pyrolytic biochar using OD was lower than that of MD, which indicated that there were other secondary reactions that consumed biochar in the pyrolytic process, such as carbon-steam reaction [36]

### 3.4 Effect of microwave drying on microwave pyrolytic biochar

To compare the pore properties of biochar using MD and OD, the specific surface area and pore parameters were tested. It can be observed from Table 4 that the specific surface area of biochar of OD was larger than that of OD. Compared with the specific surface area of TS in Table 2, the specific surface area of biochar of OD increased by 122 times, which may be caused by the release of volatiles from the TS during the pyrolytic process; the greater resistance it accumulated inside the TS, the more pores it opened up, while the specific surface area of biochar of MD had a small increase, which was three times of the MD sample, the result indicated that MD had opened up a certain amount pores of TS and the release of volatiles was peaceful with less resistance.

Figure 6 shows the scanning electron micrograph of pyrolytic biochar. As expected, the biochar obtained at different drying methods had significantly different specific surface areas and pore structures. The pore volume and average pore diameter of biochar using OD were both larger compared to MD, which was related to the release of volatiles in TS. The pores of biochar using OD were large and irregular, which was related to the violent release of volatiles in the pyrolytic

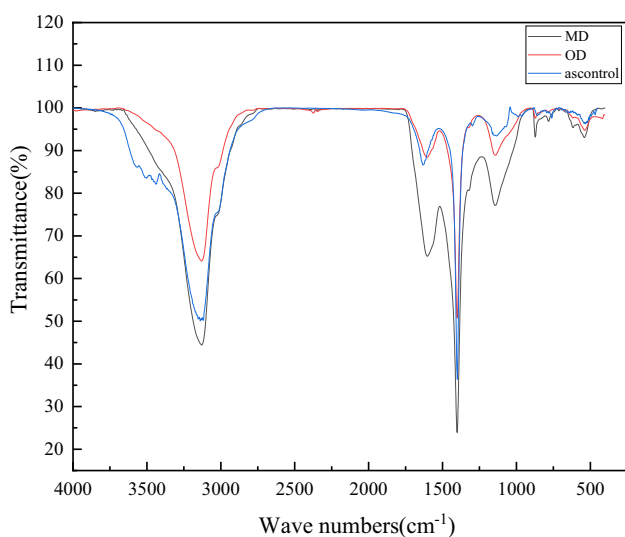


Fig. 7 FT-IR of biochar

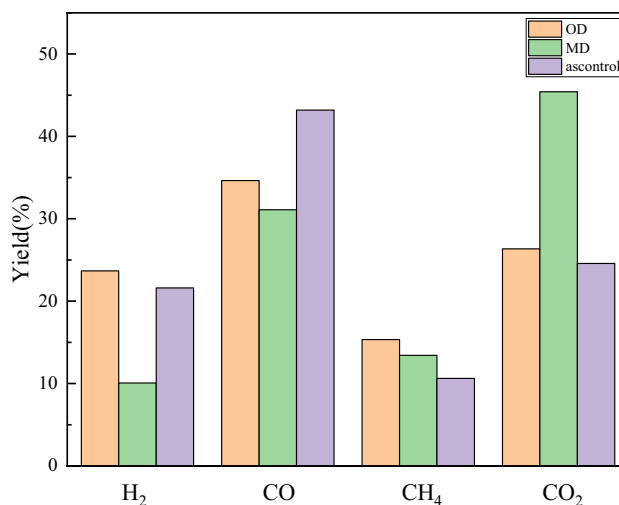


Fig. 8 Non-condensable gas yield of pyrolysis

process; it quickly destroyed the biochar surface. The pore biochar using MD was relatively regular, again verified the different release process of volatiles.

Figure 7 shows the infrared spectrum of biochar with MD, OD, and the control group. It can be seen from the infrared spectrum that there were many types of functional groups of biochar; the types of functional groups of biochar obtained by the two drying methods were roughly the same, but the strength of the functional groups was different. Such as the stretching vibration of C-H in the aromatic ring structure at 3130 cm<sup>-1</sup>, the stretching vibration of C=O at 1602Ccm<sup>-1</sup> [37], the stretching vibration of aromatic ring C=C at 1400 cm<sup>-1</sup>[38], and the asymmetric stretching vibration of C-O-C at 1140 cm<sup>-1</sup>, etc. It can be found

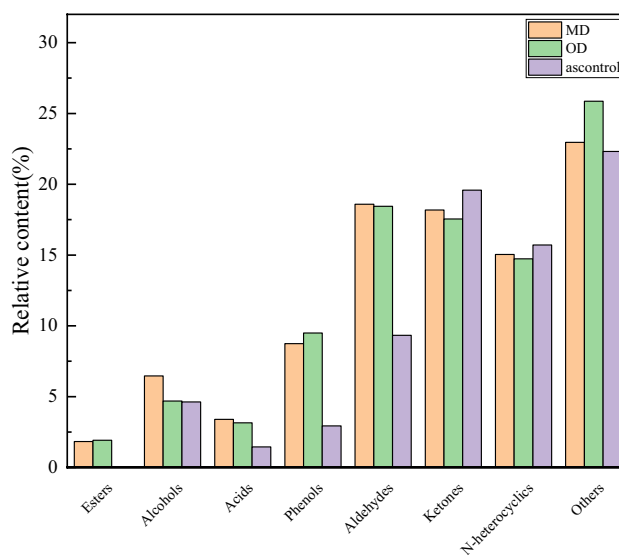


Fig. 9 Classification and relative content of bio-oil

**Table 5** Bio-oil components

Compound	Formula	Molecular weight	Peak area (%)		
			ED	MD	ascontrol
Propanoic acid	C <sub>3</sub> H <sub>6</sub> O <sub>2</sub>	74	1.74	1.62	1.45
Dihydro-2-methyl-3(2H)-furanone	C <sub>5</sub> H <sub>8</sub> O <sub>2</sub>	100	0	1.08	0
3-Hydroxy-2-butanone	C <sub>4</sub> H <sub>8</sub> O <sub>2</sub>	88	0.94	0.69	0.35
Pyrazine	C <sub>4</sub> H <sub>4</sub> N <sub>2</sub>	80	0.23	0	0
Pyridine	C <sub>5</sub> H <sub>5</sub> N	79	3.55	2.32	0.8
1-(Acetyloxy)-2-butanone	C <sub>6</sub> H <sub>10</sub> O <sub>3</sub>	130	1.39	1.11	0.73
Propanoic acid, 2-oxo-, methyl ester	C <sub>4</sub> H <sub>6</sub> O <sub>3</sub>	102	1.53	1.11	0
2-Methyl-pyridine	C <sub>6</sub> H <sub>7</sub> N	93	1.18	0.34	0
3-Aminopyridine	C <sub>5</sub> H <sub>6</sub> N <sub>2</sub>	94	1.08	0.42	0.29
Furfural	C <sub>5</sub> H <sub>4</sub> O <sub>2</sub>	96	11.50	10.46	6.15
4-Hydroxy-4-methyl-2-pentanone	C <sub>6</sub> H <sub>12</sub> O <sub>2</sub>	116	0.30	0.14	4.16
3-Furanmethanol	C <sub>5</sub> H <sub>6</sub> O <sub>2</sub>	98	2.28	1.81	4.18
1-(Acetyloxy)-2-propanone	C <sub>5</sub> H <sub>8</sub> O <sub>3</sub>	116	4.50	3.64	2.07
4-Cyclopentene-1,3-dione	C <sub>5</sub> H <sub>4</sub> O <sub>2</sub>	96	0.97	0.72	1.56
2,3-Dimethyl-pyridine	C <sub>7</sub> H <sub>9</sub> N	107	0.33	0.19	0
2-Methyl-2-cyclopenten-1-one	C <sub>6</sub> H <sub>8</sub> O	96	1.45	1.52	1.39
1-(2-Furanyl)-ethanone	C <sub>6</sub> H <sub>6</sub> O <sub>2</sub>	110	1.39	1.33	0.71
2-Hydroxy-2-cyclopenten-1-one	C <sub>5</sub> H <sub>6</sub> O <sub>2</sub>	98	0	0.72	0
Butyrolactone	C <sub>4</sub> H <sub>6</sub> O <sub>2</sub>	86	0	0	1.02
5-Methyl-2(5H)-Furanone	C <sub>5</sub> H <sub>6</sub> O <sub>2</sub>	98	0	0.17	0.55
1-Methyl-piperidine	C <sub>6</sub> H <sub>13</sub> N	99	0.13	0	0
3,5-Dimethyl-pyridine	C <sub>7</sub> H <sub>9</sub> N	407	0.83	0	0
5-Methyl-2-furancarboxaldehyde	C <sub>6</sub> H <sub>6</sub> O <sub>2</sub>	110	5.51	5.52	2.45
3-Methyl-2-cyclopenten-1-one	C <sub>6</sub> H <sub>8</sub> O	96	1.61	1.50	0.99
3-Ethenyl-pyridine	C <sub>7</sub> H <sub>7</sub> N	105	0.54	0	0
2,5-Dimethyl-2,4-dihydroxy-3(2H)-furanone	C <sub>6</sub> H <sub>8</sub> O <sub>4</sub>	144	0.27	0	0
Phenol	C <sub>6</sub> H <sub>6</sub> O	94	4.59	3.57	1.83
3,4-Dimethyl-2-cyclopenten-1-one	C <sub>7</sub> H <sub>10</sub> O	110	0	0.16	0.91
2,3-Dimethyl-cyclohexanol	C <sub>8</sub> H <sub>16</sub> O	128	0.28	0	0
2,4,6-Trimethyl-pyridine	C <sub>8</sub> H <sub>11</sub> N	121	0.17	0	0
3,6-Dimethyl-2-pyridinamine	C <sub>7</sub> H <sub>10</sub> N <sub>2</sub>	122	0.14	0	0
1H-Pyrrole-2-carboxaldehyde	C <sub>5</sub> H <sub>5</sub> NO	95	0.70	0.56	0
2-Methyl-cyclohexanone	C <sub>7</sub> H <sub>12</sub> O	112	0.12	0	0
2-Hydroxy-3-methyl-2-cyclopenten-1-one	C <sub>6</sub> H <sub>8</sub> O <sub>2</sub>	112	1.10	1.11	1.23
3,4,4-Trimethyl-5-oxo-,(E)-2-hexenoic acid	C <sub>9</sub> H <sub>14</sub> O <sub>3</sub>	170	1.29	1.06	0
2-Methyl-phenol	C <sub>7</sub> H <sub>8</sub> O	108	1.17	0.69	0.67
1-(1H-pyrrol-2-yl)-ethanone	C <sub>6</sub> H <sub>7</sub> NO	109	0.38	0.22	0
p-Cresol	C <sub>7</sub> H <sub>8</sub> O	108	1.98	2.12	0
3-Furancarboxylic acid, methyl ester	C <sub>6</sub> H <sub>6</sub> O <sub>3</sub>	126	0.39	0.52	0
Furaneol	C <sub>3</sub> H <sub>4</sub> N <sub>4</sub> O <sub>2</sub>	128	0.82	0.79	0.44
2-Methoxy-phenol	C <sub>7</sub> H <sub>8</sub> O <sub>2</sub>	124	0.96	0.89	0
3-Pyridinol	C <sub>5</sub> H <sub>5</sub> NO	95	1.32	2.88	0
2-Methyl-3-pyridinol	C <sub>6</sub> H <sub>7</sub> NO	109	0	0.33	0
3-Ethyl-2-hydroxy-2-cyclopenten-1-one	C <sub>7</sub> H <sub>10</sub> O <sub>2</sub>	126	0.33	0.30	0.42
2,3-Dihydro-3,5-dihydroxy-6-methyl-4-pyrone	C <sub>6</sub> H <sub>8</sub> O <sub>4</sub>	144	2.80	3.77	3.48
6-Methyl-3-pyridinol	C <sub>6</sub> H <sub>7</sub> NO	109	0	0.64	0
γ-Dodecalactone	C <sub>12</sub> H <sub>22</sub> O <sub>2</sub>	198	0	0.20	0
Resorcinol	C <sub>6</sub> H <sub>6</sub> O <sub>2</sub>	110	0	0.79	0
2,3-Dimethyl-phenol	C <sub>8</sub> H <sub>10</sub> O	122	0.50	0	0



**Table 5** (continued)

Compound	Formula	Molecular weight	Peak area (%)		
			ED	MD	ascontrol
2-Ethyl-phenol	C <sub>8</sub> H <sub>10</sub> O	122	0.29	0	0
5-Hydroxymethylfurfural	C <sub>6</sub> H <sub>6</sub> O <sub>3</sub>	126	0.73	2.05	0.72
2-Hydroxy-6-methyl-3-cyclohexen-1-carboxylic acid	C <sub>8</sub> H <sub>12</sub> O <sub>3</sub>	156	0	0.42	0
Hydroquinone	C <sub>6</sub> H <sub>6</sub> O <sub>2</sub>	110	0	0.68	0.43
(E)-2-Tridecanoic acid	C <sub>13</sub> H <sub>24</sub> O <sub>2</sub>	212	0	0.29	0
Nicotine	C <sub>10</sub> H <sub>14</sub> N <sub>2</sub>	162	6.55	11.78	14.62
N-Hexadecanoic acid	C <sub>16</sub> H <sub>32</sub> O <sub>2</sub>	256	0.12	0	0

from Fig. 7 that compared to OD, the peak intensities of various functional groups of biochar using MD conditions were greater, which indicated that biochar using MD had a higher degree of aromatization structure, and there were lesser volatile residues in the biochar. It was consistent with the phenomenon that the yield of bio-oil using MD was higher than that using OD in Fig. 5.

### 3.5 Analysis of non-condensable gas

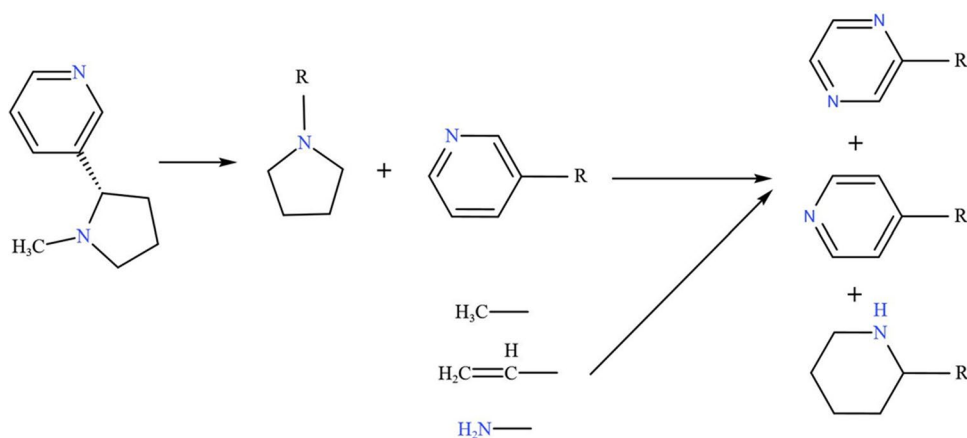
The pyrolytic gas mainly contained combustible gas with high calorific value such as CO, CH<sub>4</sub>, H<sub>2</sub>, CO<sub>2</sub>, and small molecule hydrocarbons. The component distribution of the non-condensable gases of TS is shown in Fig. 8. MD decreased the yields of H<sub>2</sub> and CO; this was because the volatiles in the reactor undergone secondary reactions such as carbon-steam, and the char reacted with steam to generate more CO and H<sub>2</sub>. Moreover, the pyrolysis of biomass can decompose H\* radicals to generate H<sub>2</sub>, and MD reduced the stay time of volatiles in the reactor. Compared to MD, OD led to a higher yield of CH<sub>4</sub> and a lower yield of CO<sub>2</sub>, mainly due to the secondary cracking of volatiles.

### 3.6 Effect of microwave drying on bio-oil properties

The components of pyrolytic bio-oil were analyzed by GC/MS to investigate the effect of MD on components of bio-oil, and the result is shown in Fig. 9. The components of bio-oil were classified as esters, alcohols, acids, phenols, aldehydes, ketones, nitrogen-containing heterocycles, and others. The contents of components were calculated to measure the area of each impurity peak and the total chromatographic peak area except the solvent peak on the chromatogram by using the area normalization method. The peak areas of each component divided by the total chromatographic peak area were the relative percentage content of each peak.

Compared to the control group (32.63%), the moisture content of the pyrolytic bio-oil using OD and MD was 20.89% and 15.25%, respectively. This was because the pretreatment of the OD promoted the degree of secondary pyrolysis and increased the number of hydroxyl broken and the generation of moisture during the pyrolytic process, also the control group. It could be observed from Fig. 9 that the relative percentage content of alcohols of MD was higher than that of OD and the control group also proved it. The aldehydes affected the quality of pyrolytic bio-oil; it was the main reason for the poor stability of the bio-oil, manifested by increased viscosity, easy oxidation, volatilization of light components, etc. The results showed that OD reduced the

**Fig. 10** Nicotine decomposition mechanism



relative content of aldehydes in the bio-oil; the content of acids and ketones also decreased, which was due to the increased residence time of volatiles in the reactor during the pyrolysis, and the oxygen-containing functional groups (carbonyl and carboxyl groups) of TS were removed more thoroughly. TS particles began to carbonize, for the most abundant K element in tobacco [23], and most of K remained in the pyrolytic biochar of TS [39]. When the volatiles diffused from the inside of TS, it was catalyzed by K [40]; K had a strong inhibitory effect on the production of aldehydes, but it improved the yield of furfural [41]. Furfural was produced by the depolymerization, ring breaking, C–C breaking, and dehydration reactions of cellulose [42]; the increase of furfural indicated that K can promote the depolymerization and dehydration of cellulose to form furfural. MD reduced the content of phenols, in addition to the sugars and polyphenols in the TS; the chlorogenic acid contained in the TS will also produce a large amount of phenols through pyrolysis [43]. OD promoted the second pyrolysis of volatiles and increases the content of phenols. The nitrogen-containing heterocycles of bio-oil were mainly composed of nicotine, pyridines, pyrazines, and piperidines. As shown in Table 5, the relative content of nicotine decreased from 11.78 (MD) to 6.55% (OD). The residence time of nicotine in the reactor was prolonged, and it is decomposed at high temperature to generate nitrogen-containing heterocyclic free radicals and combine with free radicals generated by the decomposition of other substances to generate pyridines, pyrazines, and piperidines (Fig. 10).

## 4 Conclusions

In this work, the drying characteristics and effect on microwave pyrolysis of TS using volumetric heating were investigated and compared with surface heating. The drying curves, the TG-DTG curves, and the pyrolytic products were also analyzed and studied. The main conclusions were as follows:

- (1) The drying speed at microwave power at 540 W was about 5 times than that of OD at 105°C, and the specific surface area and porosity of TS increased using MD, which helped to quickly release volatiles during the pyrolytic process of TS. The residence time in the reactor reduced, and the degree of secondary cracking of the volatiles matter lowered.
- (2) The weight loss of TS decreased using MD, compared with OD, at every temperature point from 50 to 1200 °C. At the range of temperature from 220 to 375°C, the DTG curve had obviously main peak and shoulder peak; MD increased the peak value of shoulder peak, and opposite the main peak. MD tinily

affected the second half of the DTG curve, and the second half of curve almost overlaps together.

- (3) The yields of H<sub>2</sub>, CO, and CH<sub>4</sub> decreased using MD, which was caused by the secondary reaction of volatiles in the reactor. The degree of secondary pyrolysis of volatiles lowered, and the moisture content of bio-oil was lowered. The relative content of alcohols and nitrogen-containing heterocyclic components increased, and the relative content of acids, aldehydes, and ketones also increased, which was the reason that the residence time of volatiles in the reactor decreased. Nicotine was thermally decomposed and combined with other free radicals at high temperature and oxygen-free environment to form nitrogen-containing heterocyclic components (pyridines, pyrazines, and piperidines) with smaller molecular weight.

**Funding** This work was supported by the National Natural Science Fund of China (grant number NSFC- 52006200); the National Innovation and Entrepreneurship Program for College Students (item number: 202010459058); and the Program of Biomass Resources Processing and Efficient Utilization of Outstanding Foreign Scientists' Workroom (grant number GZS2018004).

## Declarations

**Conflict of interest** The authors declare no competing interests.

## References

1. Gwenzi W, Chaukura N, Wenga T, Mtisi M (2021) Biochars as media for air pollution control systems: contaminant removal, applications and future research directions. *Sci Total Environ* 753:142249
2. Shan R, Han J, Gu J, Yuan H, Luo B, Chen Y (2020) A review of recent developments in catalytic applications of biochar-based materials. *Resour Conserv Recycl* 162:105306
3. Pandey B, Prajapati YK, Sheth PN (2019) Recent progress in thermochemical techniques to produce hydrogen gas from biomass: a state of the art review. *Int J Hydrogen Energy* 44(47):25384–25415
4. Huber GW, Iborra S, Corma A (2006) Synthesis of transportation fuels from biomass: chemistry, catalysts, and engineering. *Chem Rev* 106(9):4044–4098
5. Xiu S, Shahbazi A (2012) Bio-oil production and upgrading research: a review. *Renew Sustain Energy Rev* 16(7):4406–4414
6. Wang D, Li DB, Liu YQ, Lv DC, Ye YY, Zhu SJ, Zhang BB (2014) Study of a new complex method for extraction of phenolic compounds from bio-oils. *Sep Purif Technol* 134:132–138
7. Mante OD, Thompson SJ, Mustapha S, Dayton DC (2019) A selective extraction method for recovery of monofunctional methoxyphenols from biomass pyrolysis liquids. *Green Chem* 21(9):2257–2265

8. Fu D, Farag S, Chaouki J, Jessop PG (2014) Extraction of phenols from lignin microwave-pyrolysis oil using a switchable hydrophilicity solvent. *Bioresour Technol* 154:101–108
9. Pang SS, Mujumdar AS (2010) Drying of woody biomass for bioenergy: drying technologies and optimization for an integrated bioenergy plant. *Dry Technol* 28(5):690–701
10. Di Blasi C (1998) Multi-phase moisture transfer in the high-temperature drying of wood particles. *Chem Eng Sci* 53(2):353–366
11. A WHC, B JP, B XTBJR (2015) Reviews SE: A state-of-the-art review of biomass torrefaction, densification and applications. *Renew Sust Energ Rev* 44:847–866
12. Li J, Li N, Qiao Y, Zong P, Wang C, Tian Y, Qin SJICSE, Science E (2020) Biomass pyrolysis liquefaction technique: state of research and development trends. *558(2):022016 (022019pp)*
13. Lenaerts S, Van Der Borgh M, Callens A, Van Campenhout L (2018) Suitability of microwave drying for mealworms (*Tenebrio molitor*) as alternative to freeze drying: Impact on nutritional quality and colour. *Food Chem* 254:129–136
14. Qu F, Zhu X, Ai Z, Ai Y, Qiu F, Ni D (2019) Effect of different drying methods on the sensory quality and chemical components of black tea. *Lwt* 99:112–118
15. Menéndez JA, Inguanzo M, Pis JJJWR (2002) Microwave-induced pyrolysis of sewage sludge. *Water Res* 36(13):3261–3264
16. Kumar AK, Sharma S (2017) Recent updates on different methods of pretreatment of lignocellulosic feedstocks: a review. *Bioresour Bioprocess*. 4(1):7
17. Chen C, Yang S, Bu X (2019) Microwave drying effect on pyrolysis characteristics and kinetics of microalgae. *Bioenerg Res* 12(2):400–408
18. Huang YF, Chen WR, Chiueh PT, Kuan WH, Lo SLJBT (2012) Microwave torrefaction of rice straw and pennisetum. *Bioresour Technol* 123:1–7
19. Zhou G, Huang Q, Yu B, Tong H, Chi Y, Yan JJJoCE (2017) Effect of industrial microwave irradiation on the physicochemical properties and pyrolysis characteristics of lignite. *Chinese J Chem Eng* 26(5):1171–1178
20. Mina AR, Tecson B, Virtucio DV, Felix C, Garibay S (2017) Optimization of microwave drying of microalgae *Nannochloropsis* sp. for biofuel production. In: 2017 IEEE 9th International Conference on Humanoid, Nanotechnology, Information Technology, Communication and Control, Environment, and Management (HNICEM) 1-3 Dec. 2017, pp 1-5
21. Wang X, Chen H, Luo K, Shao J, Yang H (2008) The influence of microwave drying on biomass pyrolysis. *Energy Fuels* 22(1):67–74
22. Zi W, Chen Y, Pan Y, Zhang Y, He Y, Wang Q (2019) Pyrolysis, morphology and microwave absorption properties of tobacco stem materials. *Sci Total Environ* 683:341–350
23. Chen Z, Leng E, Zhang Y, Zheng A, Peng Y, Gong X, Huang Y, Qiao Y (2018) Pyrolysis characteristics of tobacco stem after different solvent leaching treatments. *J Anal Appl Pyrol* 130:350–357
24. Liu B, Li Y-M, Wu S-B, Li Y-H, Deng S-S, Xia Z-L (2013) Pyrolysis characteristic of tobacco stem studied by Py-GC/MS, TG-FTIR, and TG-MS. *BioResources* 8(1):220–230
25. Zhou G, Huang Q, Yu B, Tong H, Chi Y, Yan J (2018) Effect of industrial microwave irradiation on the physicochemical properties and pyrolysis characteristics of lignite. *Chin J Chem Eng* 26(5):1171–1178
26. Villagrancia ARC, Mayol AP, Ubando AT, Biona JBMM, Arboleda NB, David MY, Tumlos RB, Lee H, Lin OH, Espiritu RA et al (2016) Microwave drying characteristics of microalgae (*Chlorella vulgaris*) for biofuel production. *Clean Technol Environ Policy* 18(8):2441–2451
27. Amer M, Nour M, Ahmed M, Ookawara S, Nada S, Elwardany A (2019) The effect of microwave drying pretreatment on dry torrefaction of agricultural biomasses. *Bioresour Technol* 286:121400
28. Chen X, Liu L, Zhang L, Zhao Y, Xing C, Jiao Z, Yang C, Qiu P (2021) Effect of active alkali and alkaline earth metals on physicochemical properties and gasification reactivity of co-pyrolysis char from coal blended with corn stalks. *Renew Energy* 171:1213–1223
29. Verma R, Verma SK, Verma S, Wang J, Liu J, Jing B, Rakesh KP (2021) Value-addition of wheat straw through acid treatment and pyrolysis of acid treated residues. *J Clean Prod* 282:124488
30. Rizwan M, Lin Q, Chen X, Li Y, Li G, Zhao X, Tian Y (2020) Synthesis, characterization and application of magnetic and acid modified biochars following alkaline pretreatment of rice and cotton straws. *Sci Total Environ* 714:136532
31. Rahman MS, Perera COJCP (2007) Handbook of food preservation, Second Edition. CRC Press, (Part C)
32. Müsellim E, Tahir MH, Ahmad MS, Ceylan S (2018) Thermokinetic and TG/DSC-FTIR study of pea waste biomass pyrolysis. *Appl Therm Eng* 137:54–61
33. Zeynep YLZ, Selim CJoTA, Calorimetry (2018) Pyrolysis of tobacco factory waste biomass: TG-FTIR analysis, kinetic study and bio-oil characterization. *J Therm Anal Calorim* 136:783–794
34. Liew RK, Nam WL, Chong MY, Phang XY, Su MH, Yek PNY, Ma NL, Cheng CK, Chong CT, Lam SS (2018) Oil palm waste: an abundant and promising feedstock for microwave pyrolysis conversion into good quality biochar with potential multi-applications. *Process Saf Environ Prot* 115:57–69
35. Ahuja P, Kumar S, Singh PCJCE, Technology (2010) A model for primary and heterogeneous secondary reactions of wood pyrolysis. *19(3):272-282*
36. Graham RG (1993) A characterization of the fast pyrolysis of cellulose and wood biomass. The University of Western Ontario (Canada), Digitized Theses. 2292
37. Abedi A, Cheng H, Dalai AK (2018) Effects of natural additives on the properties of sawdust fuel pellets. *Energy Fuels* 32(2):1863–1873
38. Özçimen D, Ersoy-Meriçboyu A (2010) Characterization of biochar and bio-oil samples obtained from carbonization of various biomass materials. *Renew Energy* 35(6):1319–1324
39. Leijenhorst EJ, Wolters W, van de Beld L, Prins W (2016) Inorganic element transfer from biomass to fast pyrolysis oil: review and experiments. *Fuel Process Technol* 149:96–111
40. Galgano A, Di Blasi C (2004) Modeling the propagation of drying and decomposition fronts in wood. *Combust Flame* 139(1):16–27
41. Zhang H, Ma Y, Shao S, Xiao RJAE (2017) The effects of potassium on distributions of bio-oils obtained from fast pyrolysis of agricultural and forest biomass in a fluidized bed. *Appl Energy* 208:867–877
42. Zhang H, Liu X, Lu M, Hu X, Lu L, Tian X, Ji J (2014) Role of Brønsted acid in selective production of furfural in biomass pyrolysis. *Biores Technol* 169:800–803
43. Wang Z, Li X, Zhen S, Li X, Wang C, Wang Y (2013) The important role of quinic acid in the formation of phenolic compounds from pyrolysis of chlorogenic acid. *J Therm Anal Calorim* 114(3):1231–1238

**Publisher's note** Springer Nature remains neutral with regard to jurisdictional claims in published maps and institutional affiliations.